

Transcriptome analysis reveals new insights into MdBAK1-mediated plant growth in *Malus domestica*

Liwei Zheng, Yingli Yang, Cai Gao, Juanjuan Ma, Kamran Shah, Dong
Zhang, Caiping Zhao, Libo Xing, Mingyu Han, na an, and Xiaolin Ren

J. Agric. Food Chem., **Just Accepted Manuscript** • DOI: 10.1021/acs.jafc.9b02467 • Publication Date (Web): 02 Aug 2019

Downloaded from pubs.acs.org on August 3, 2019

Just Accepted

“Just Accepted” manuscripts have been peer-reviewed and accepted for publication. They are posted online prior to technical editing, formatting for publication and author proofing. The American Chemical Society provides “Just Accepted” as a service to the research community to expedite the dissemination of scientific material as soon as possible after acceptance. “Just Accepted” manuscripts appear in full in PDF format accompanied by an HTML abstract. “Just Accepted” manuscripts have been fully peer reviewed, but should not be considered the official version of record. They are citable by the Digital Object Identifier (DOI®). “Just Accepted” is an optional service offered to authors. Therefore, the “Just Accepted” Web site may not include all articles that will be published in the journal. After a manuscript is technically edited and formatted, it will be removed from the “Just Accepted” Web site and published as an ASAP article. Note that technical editing may introduce minor changes to the manuscript text and/or graphics which could affect content, and all legal disclaimers and ethical guidelines that apply to the journal pertain. ACS cannot be held responsible for errors or consequences arising from the use of information contained in these “Just Accepted” manuscripts.

1 **Transcriptome analysis reveals new insights into *MdBAK1*-mediated plant growth in *Malus***
2 ***domestica***

3

4 Liwei Zheng,[†] Yingli Yang,[†] Cai Gao,[†] Juanjuan Ma,[†] Kamran Shah,[†] Dong Zhang,[†] Caiping Zhao,[†]

5 Libo Xing,[†] Mingyu Han,[†] Na An,^{*,†,‡} and Xiaolin Ren^{*,†}

6

7 [†] College of Horticulture, Northwest A & F University, Yangling, Shaanxi 712100, China

8 [‡] College of Life Science, Northwest A & F University, Yangling, Shaanxi 712100, China

9 **ABSTRACT:** *BAK1* effects on plant stress responses have been well documented, but little is known
10 regarding its effects on plant growth. In this study, we functionally characterized *MdBAK1*.
11 Overexpressing *MdBAK1* in *Arabidopsis thaliana* and apple trees promoted growth. Longitudinal stem
12 cells were longer in transgenic plants than in wild-type plants. The size and number of cells and the
13 area of the transverse stem were greater in the transgenic lines than in the wild-type plants. Moreover,
14 transgenic *A. thaliana* and apple plants were more sensitive to an exogenous brassinosteroid. A
15 transcriptome analysis of wild-type and transgenic apple revealed that *MdBAK1* overexpression
16 activated the brassinosteroid and ethylene signals, xylem production, and stress responses. Trend and
17 Venn analyses indicated that carbohydrate, energy, and hormone metabolic activities were greater in
18 transgenic plants during different periods. Moreover, a weighted gene co-expression network analysis
19 proved that carbohydrate, hormone, and xylem metabolism as well as cell growth may be critical for
20 *MdBAK1*-mediated apple tree growth and development. Compared with the corresponding levels in
21 wild-type plants, the endogenous brassinosteroid, cytokinin, starch, sucrose, trehalose, glucose,
22 fructose, and total sugar contents were considerably different in transgenic plants. Our results imply
23 that *MdBAK1* helps to regulate growth of apple tree through the above-mentioned pathways. These
24 findings provide new information regarding the effects of *MdBAK1* on plant growth and development.

25 **KEYWORDS:** *Brassinosteroid, MdBAK1, Malus domestica, growth and development, RNA-seq*

26 INTRODUCTION

27 Brassinosteroids (BRs) comprise a class of plant-specific steroid hormones that promote plant growth
28 and development by regulating cell differentiation, expansion and proliferation. Furthermore, it is also
29 involved in efficient plant architecture, xylem differentiation and stress responses.¹⁻³ The biological

30 functions of BRs are inseparable from the BR signal regulatory network. The BR signal transduction
31 pathway has been identified in *Arabidopsis thaliana*.⁴ The underline mechanism revealed that BR
32 signal is first perceived by BRI1 and BAK1, which dissociates the BRI1-BKI1 complex and activates
33 BRI1. The activated BRI1 induces BSK1 to repress BIN2, resulting in the accumulation of active
34 BZR1/2 in the nucleus. Finally, transcription factors BZR1/2 affect the expression of target genes
35 associated with the regulation of plant growth and development. The *BRI1*, *BSU1*, and *BSK* genes
36 influence stem elongation, apical dominance, and leaf growth.² The phenotypes of the gain-of-function
37 mutants *bki1-D* and *bin2-D* are similar to those of mutants lacking *BRI1*. A previous study revealed
38 that AtBKI1 interacts with ERECTA to regulate plant architecture.⁵ Moreover, AtBIN2 represses
39 cellulose synthesis by phosphorylating cellulose synthase 1,⁶ whereas BZR1 interacts with SMALL
40 ORGAN SIZE1 to regulate BR signaling and plant architecture.⁷

41 *Arabidopsis thaliana* and rice contain one *BAK1* gene.⁸ This gene, which is also called *SERK3*, was
42 identified via two-hybrid screening and activation label screening.⁸ Additionally, *BAK1* encodes a BR
43 receptor which is involved in the plant innate immune response, cell death, and abiotic stress
44 responses.⁹ For example, bacterial flagellin induces BAK1 and FLAGELLIN-SENSITIVE 2 to form a
45 complex.⁹ Moreover, BAK1 directly interacts with AvrPto and AvrPtoB, which initiates
46 effector-triggered immunity.¹⁰ An earlier investigation confirmed that BAK1-mediated cell death
47 requires BAK1-interacting receptor-like kinase 1 and 3.¹⁰ The BAK1-BON1 protein complex
48 contributes to temperature-mediated growth and cell death.¹¹ Furthermore, BAK1,
49 BOTRYTIS-INDUCED KINASE1, and U-box E3 ubiquitin ligases PUB12 and PUB13, take high
50 participation in plant innate immune responses.¹²

51 Previous studies proved that BR signal-related genes are associated with plant growth and some

52 important agronomic traits, whereas *BAK1* is essential for plant stress responses.² As the co-receptor of
53 BRI1, BAK1 likely to affects these agronomic traits, but its precise effects on these traits need to be
54 confirmed. Apple is a dominant temperate perennial fruit tree, and its vegetative growth stage is closely
55 related to fruit bearing, yield, and quality. Therefore, characterizing *MdBAK1* will expand the available
56 information regarding plant *BAK1* genes and may be relevant for the generation of new apple varieties.

57 In this study, *MdBAK1* was cloned and overexpressed in *A. thaliana* and *Malus domestica*. The
58 growth and biomass of wild-type (WT) and transgenic plants were compared. There was an obvious
59 difference in the anatomical stem structure between the WT and transgenic plants. The sensitivity of
60 the WT and transgenic lines to exogenous BR was assessed. Moreover, RNA-sequencing (RNA-seq)
61 was used to analyze the transcriptome changes in WT and transgenic apple. The metabolic pathways
62 were characterized through a comparative analysis and trend and Venn analyses of each genotype. A
63 weighted gene co-expression network analysis (WGCNA) was used to define modules and genes that
64 were highly correlated with growth traits. The pivotal physiological indices, including hormone and
65 sugar contents, were also measured. The findings described herein represent new information regarding
66 *MdBAK1*-mediated growth and development in apple tree.

67 **MATERIALS AND METHODS**

68 **Plant materials, gene cloning, and subcellular localization.** Various tissues [shoot tip (ST),
69 xylem of young stem (YX), phloem of young stem (YP), xylem of mature stem (MX), phloem of
70 mature stem (MP), juvenile leaves (JL), mature leaves (ML), and new roots (R)] were harvested from
71 1-year-old dwarf apple rootstock [Malling 9-T337 (M.9-T337)]. Each sample was replicated thrice by
72 taking sample from three different trees per group (three trees per replicate). The ST was collected
73 from trees treated with BR (Sigma Chemical Co., Deisenhofen, Germany) as previously described.³ In
74 a tissue culture room, *Malus prunifolia* was cultured on Murashige and Skoog (MS) agar medium
75 containing 0.1 mg/L brassinolide (BL). The ST of *M. prunifolia* seedlings were sampled at 0, 7, 14, 28,
76 and 42 days after the BR treatment.

77 The *MdBAK1* (MD15G1412700) coding sequence was amplified with gene-specific primers (Table
78 S1) and cDNA from the ST of M.9-T337 as the template. The amplified fragment was ligated into the
79 pMD19-T vector (Takara, Dalian, China) and sequenced. Sequences were aligned with the DNAMAN
80 program. The MEGA 7 software was used to construct a phylogenetic tree, with 1,000 bootstrap
81 replicates.¹³ Plant-mPLoc (<http://www.csbio.sjtu.edu.cn/bioinf/plant-multi/>) was used to predict the
82 subcellular localization of MdBAK1. The *MdBAK1* coding sequence without the termination codon
83 was introduced into the pCAMBIA1302 vector (<http://www.cambia.org>) for the production of a fusion
84 protein with a green fluorescent protein (GFP) tag. The recombinant plasmid was sequenced and then
85 inserted into *Agrobacterium tumefaciens* cells, which were then used to transform *Nicotiana*
86 *benthamiana* leaf cells. The transgenic tobacco plants were grown for an additional 72 h at 21–23 °C
87 under a 16-h photoperiod. The GFP signals were observed with the A1R/A1 confocal microscope

88 (Nikon, Tokyo, Japan).

89 **Construction of a plant *MdBAK1* overexpression vector for the transformation of *Arabidopsis***

90 ***thaliana* and apple.** The *MdBAK1* coding sequence without the termination codon was inserted into
91 pCAMBIA1301 (GUS-flag) and pCAMBIA2300 (GFP-flag) vectors, which respectively contained the
92 hygromycin (hygII) and kanamycin (nptII) resistance markers. *Arabidopsis thaliana* Columbia (Col-0)
93 was transformed with *A. tumefaciens* strain EHA105 cells harboring pCAMBIA1301-*MdBAK1*
94 according to the floral dip method.¹⁴ Putative transgenic *A. thaliana* plants were selected on MS agar
95 medium containing 50 mg/l hyg II. The surviving plants were analyzed by PCR to confirm they were
96 correctly transformed. A quantitative real-time (qRT)-PCR assay was used to confirm *MdBAK1* was
97 expressed in the transgenic *A. thaliana* plants.

98 Transgenic GL3 apple lines were generated from leaf fragments through *A. tumefaciens*-mediated
99 transformation with pCAMBIA2300-*MdBAK1*. The npt II -resistant buds were sub-cultured every 2
100 months on MS medium containing 50 mg/l npt II. False-positive buds were eliminated, after which the
101 buds that grew normally were verified by PCR and qRT-PCR. Moreover, *MdBAK1* abundance was
102 assessed with the FluoView FV1000 confocal microscope (Olympus Corp., Tokyo, Japan). Images
103 were captured with a digital camera (Olympus Corp.) attached to the microscope.¹⁵

104 **Growth indices, histological examination, and endogenous hormone and sugar measurements.**

105 Plant height (PH), stem diameter, average internode length, stem fresh and dry weights, leaf fresh and
106 dry weights, leaf area, and root length were measured as previously described.³ A histological analysis
107 was performed, and samples were observed with a BX51 microscope (Olympus Corp.) equipped with a
108 digital camera to photograph sections. Cell size and number were determined with the Image
109 Processing and Analysis in Java 1.41 (Image-Pro Plus 6.0) software.

110 The ST endogenous BL and cytokinin (CTK) contents were quantified with an enzyme-linked
111 immunosorbent assay, which was conducted at the Phytohormones Research Institute (China
112 Agricultural University) as previously described.³ The BL content was determined by
113 high-performance liquid chromatography-mass spectrometry (HPLC-MS) at ZooNBIO
114 BioTECHNOLOGY (Nanjing, China). The ST soluble sugar and starch contents were analyzed by
115 HPLC (Waters 2414, Visible Detector, Shaanxi, China).¹⁶

116 **Brassinosteroid treatment of transgenic *Arabidopsis thaliana* and apple.** Surface-sterilized Col-0
117 seeds were sown on half-strength MS medium containing 0 or 100 nM BR, and then incubated in
118 darkness at 4 °C for 4 days. The resulting seedlings were grown under light at 22 °C for 7 days, after
119 which the roots were photographed and their length was measured.¹ The sensitivity of 2-month-old
120 GL3 apple seedlings to BR was assessed after BR (0 and 3.0 mg/l) treatments.³

121 **RNA extraction, qRT-PCR, RNA sequencing, and DNA isolation.** Total RNA was isolated
122 according to a CTAB method¹⁷ for a subsequent qRT-PCR assay, which was performed with
123 gene-specific primers (Table S1). The apple *EF-1 α* gene (GenBank accession no. DQ341381)³ and the
124 *A. thaliana* TUB gene were respectively used as reference standards for gene expression analyses of
125 apple and *A. thaliana*. For the transcriptome assembly, 18 cDNA libraries were constructed for the WT
126 and MdBAK1-OX#5 (B) STs (i.e., three time-points, with three biological replicates). The libraries
127 were sequenced with the HiSeq 4000 system (Illumina, San Diego, CA, USA) at the Genedenovo
128 Company (Guangzhou, China). Genomic DNA was extracted to detect transformed *A. thaliana* and
129 apple plants according to a modified CTAB method.

130 **RNA-sequencing data analysis.** Reads with adapter sequences, more than 10% unknown bases, or
131 low-quality bases were eliminated. Additionally, rRNAs were removed with the Bowtie program
132 (version 2.2.8).¹⁸ The high-quality clean reads were mapped to the apple genome GDDH13 sequence
133 (version 1.1) (<https://www.rosaceae.org/>)¹⁹ with TopHat2 (version 2.1.1).²⁰ Novel genes were identified
134 and annotated with the Cufflinks (version 2.2.1) reference annotation-based transcript assembly
135 method.

136 The number of fragments per kilobase of transcript per million mapped reads for genes was

137 calculated as previously described.²¹ Pearson's correlation coefficients were determined with R
138 (<http://www.r-project.org/>). Differentially expressed genes (DEGs) [i.e., $FDR < 0.05$ and $|\log_2$
139 $(\text{fold-change})| \geq 1$] were identified with the edgeR package (version 3.12.1) (<http://www.r-project.org/>).
140 The DEGs were clustered with the Short Time-series Expression Miner (STEM) software
141 (<http://www.cs.cmu.edu/~jernst/stem/>). The DEGs with similar expression patterns were included in
142 the same profile. The profiles with $p < 0.05$ were identified as significantly enriched modules. A Venn
143 analysis was completed with DEGs over time. The WGCNA software package (version 1.51) in R was
144 used to construct highly co-expressed gene modules with high-quality genes, which were expressed in
145 more than half of the samples.²² A topological overlap matrix was used for constructing a WGCNA
146 network and detecting modules (minimum size of 50 and a mergeCutHeight of 0.3). Associations
147 between modules and traits [PH, stem diameter (SD), leaf fresh weight (LFW), and primary shoot
148 growth rate (PSGR)] were evaluated with all genes in each module. Significant trait-related modules
149 were identified based on high correlation values and $p < 0.05$. The genes related to specific traits in
150 significant modules were used to construct co-expression networks via the Cytoscape 3.5 software.²³

151 A gene ontology (GO) analysis was performed with the Goseq R package
152 (<http://www.r-project.org/>). Additionally, a Kyoto Encyclopedia of Genes and Genomes (KEGG)
153 pathway enrichment analysis was completed with the KOBAS web server
154 (<http://kobas.cbi.pku.edu.cn/>). A corrected p -value ≤ 0.05 was used as the threshold for significance.
155 Novel genes were annotated and functionally classified with WEGO software.

156 **Statistical analysis.** Data were analyzed with the Statistical Product and Service Solutions (SPSS)
157 software (IBM Co., Armonk, USA).

158 RESULTS

159 **Molecular cloning and analysis of the sequence and expression of *MdBAK1* as well as the**
160 **subcellular localization of the encoded protein.** To functionally characterize *MdBAK1*, we cloned
161 *MD15G1412700*. We revealed that the gene comprises 1,851 bp and encodes 616 amino acids. The
162 deduced protein sequence and BAK1 protein sequences from other species contained 10 conserved
163 domains, including a signal peptide, a putative leucine zipper, five leucine-rich repeats (LRRs), a
164 proline-rich domain, a transmembrane region, and a serine/threonine kinase domain, as well as several
165 conserved function-related sites (e.g., D122, K317, C408, D416, D434, and T455) (Figure S1a).
166 Additionally, MD15G1412700 was highly similar to *Prunus avium* BAK1 (PaBAK1) (Figure S1b).
167 Therefore, *MD15G1412700* in apple was named *MdBAK1*.

168 The *MdBAK1* gene was expressed in all tissues, but highly expressed in JL, ML, and YX (Figure
169 S2a). The BR treatment respectively increased *MdBAK1* expression by about 4.2-, 1-, 5-, and 4.5-fold
170 at 30, 60, 90, and 120 min (Figure S2b). Moreover, *MdBAK1* expression was also respectively induced
171 by about 4.5-, 0.8-, 1.2-, and 1-fold by BR at 0, 14, 28, 42, and 56 days (Figure S2c). HPLC analysis
172 showed that the BR level was about 12-fold higher in treated STs than in control STs at 14 days (Figure
173 S3). Furthermore, *M. prunifolia* growth was enhanced by BR (Figure S4a). Plant height, average
174 internode length, number of nodes, shoot fresh weight, LFW, and leaf area respectively increased by
175 about 1.5 cm, 0.14 cm, 0, 0.09 g, 0.07 g, and 0.5 cm² at 42 days after the BR treatment (Figure S4b). In
176 *M. prunifolia*, *MdBAK1* expression was significantly upregulated at 0, 7, 14, and 42 days after the BR

177 treatment (Figure S2d).

178 The subcellular localization of a protein is important for its function. We predicted that MdBAK1
179 localizes in the cell membrane. To verify this prediction, the 35S::*MdBAK1-GFP* and 35S::*GFP*
180 (negative control) constructs were inserted into tobacco leaves. The observed fluorescence confirmed
181 our prediction that MdBAK1 was localized in cell membrane (Figure S5).

182

183 **Effect of *MdBAK1* overexpression on growth and development.** The *MdBAK1* coding sequence
184 under the control of the CaMV35S promoter was inserted into Col-0 plants (Figure S6a). Seven
185 independent transgenic lines were analyzed by PCR with primers specific for the hygII resistance
186 marker (Figure S6b). Lines #1, #3, and #4, which had the highest *MdBAK1* levels, were selected for
187 further experiments (Figure S6c).

188 The transgenic apple plants were transformed with the *MdBAK1* and *GFP* fusion construct under the
189 control of the CaMV35S promoter (Figure S7a). Six transgenic apple plants were obtained and then
190 analyzed by PCR with primers specific for the nptII resistance marker (Figure S7b). Western blot
191 revealed a high MdBAK1 protein level in transgenic plants (Figure S7c). Additionally, the *MdBAK1*
192 transcript level in transgenic lines was 3- to 10-fold higher than that in WT plants (Figure S7d).
193 Transgenic plants with the highest *MdBAK1* expression levels (lines #1, #2, and #5) were analyzed
194 further.

195 At 21 days after transplanting, *MdBAK1*-overexpressing *A. thaliana* plants (lines #1, #3, and #4)
196 were taller and had larger leaves compared with WT plants (Figure S8a). Additionally, compared with
197 the WT plants, the 45-day-old transgenic plants resulted in an increased biomass (Figure S8b), and

198 their PH, average internode length, number of nodes, stem diameter, whole seedling weight, and shoot
199 weight were respectively greater by about 4–6 cm, 0.4–0.6 cm, 0.6–1, 0.2–0.5 mm, 0.09–0.13 g, and
200 0.013–0.027 g (Figure S8c). To further explore the influence of *MdBAK1* over-expression on plant
201 growth, we compared the anatomical structures of the transgenic and WT plants. Pith cells were
202 significantly larger in the transgenic plants relative to WT (Figure 1a), and the pith cells were about
203 20–40 μm longer in the transgenic plants than in the WT plants (Figure 1b). The stem area was
204 respectively 0.17, 0.51, 0.54, and 0.49 mm^2 in the WT, #1, #3, and #4 plants (Figure 1c and Table 1).
205 Xylem area and cell size were enhanced in the transgenic plants (Table 1). There were more xylem
206 cells in #1 and #4 plants than in WT plants, whereas there were no obvious differences between #3
207 plants and the WT controls (Table 1). The phloem area of the transgenic lines was about 3- to 6-fold
208 greater than that of the WT plants (Table 1). The phloem cells were respectively 14.25, 94.23, 70.22,
209 and 65.55 μm^2 in the WT, #1, #3, and #4 plants. In contrast, the number of phloem cells was unaffected
210 by *MdBAK1* overexpression (Table 1). The pith area was respectively 46,277.43, 206,370.25,
211 173,869.32, and 232,083.16 μm^2 in the WT, #1, #3, and #4 plants. The pith cells were about 4- to
212 5-fold larger in the transgenic lines than in the WT plants (Table 1); however, there were no differences
213 in the number of pith cells (Table 1). The proportion of pith cells was about 5% to 20% greater in the
214 *MdBAK1*-overexpressing plants than in the WT plants (Figure 1d). The percentages of xylem and
215 phloem were 2.64% and 1.64% in WT plants, 4.02% and 3.69% in #1 plants, 2.67% and 2.67% in #3
216 plants, and 2.99% and 2.7% in #4 plants. Differences among the analyzed transgenic lines and WT
217 plants were also detected for other components (Figure 1d). To clarify the role of *MdBAK1* during BR
218 signaling, we performed a root growth inhibition assay. The transgenic lines were more sensitive to BR
219 (Figure 2a), which respectively decreased root length by about 15, 23, 24, and 26 mm in the WT, #1,

220 #3, and #4 plants (Figure 2b).

221 We also examined the effects of *MdBAK1* on apple tree growth and development. One-month-old
222 transgenic apple seedlings grew more vigorously than WT seedlings (Figure S9a), with the fresh
223 weight of transgenic seedlings about 0.15–0.2 g greater than that of the WT seedlings (Figure S9b). An
224 analysis of plants grown in a greenhouse for 2 months revealed that the transgenic plants grew faster
225 than the WT plants (Figure S10a). The #1, #2, and #5 plants were respectively 2.7, 2.5, and 4.9 cm
226 taller than the WT plants. The stem diameter of WT plants was about 0.6–0.9 cm smaller than that of
227 the transgenic plants. The average internode length of WT, #1, #2, and #5 plants was respectively about
228 0.18, 0.3, 0.29, and 0.31 cm. The stem fresh and dry weights were obviously greater in the transgenic
229 lines, as were the leaf dry and fresh weights and leaf area (Figure S10b). The phenotypic differences
230 were greater among 5-month-old plants (Figure S10c). The #1, #2, and #5 plants were respectively
231 about 25, 28, and 34 cm taller than the WT plants. The main stem of the transgenic plants was about
232 0.9–1.3 mm thicker than that of the WT plants. The average internode length, stem fresh and dry
233 weights, and leaf biomass (leaf fresh and dry weights and area) were also greater in the transgenic
234 plants compared to WT plants (Figure S10d).

235 To more precisely characterize the effect of *MdBAK1* on plant growth, we dissected the stems of
236 5-month-old transgenic and wild-type apple plants. An examination of the longitudinal structure
237 revealed that the xylem, phloem, pith, and cortical cells were longer in the transgenic trees than in the
238 WT trees (Figure 3a and Table 2). The xylem cells were respectively about 13, 67, and 111 μm shorter
239 in the WT trees than in the #1, #2, and #5 trees (Table 2). Regarding the WT, #1, #2, and #5 trees, the
240 phloem cell length was respectively 70.21, 87.39, 113.62, and 120.81 μm (Table 2), and the pith cell
241 length was respectively 30.47, 54.66, 82.87, and 83.54 μm . The cortical cells were about 24, 48, and 49

242 μm longer in the transgenic apple trees than in the WT trees (Table 2). The stem area (5 cm above
243 ground) was respectively 4.34, 10.37, 11.00, and 11.63 mm^2 in the WT, #1, #2, and #5 trees (Figure 3b
244 and Table 3). The xylem thickness was respectively 1.41, 2.41, 3.13, and 3.97 mm^2 in the WT, #1, #2,
245 and #5 trees. The xylem cells of #1, #2, and #5 trees were about 101, 84, and 101 μm^2 larger than those
246 of the WT trees. Moreover, the #2 and #5 trees had more xylem cells than the WT trees, whereas the
247 opposite pattern was observed for #1 trees (Table 3). A comparison of WT, #1, #2, and #5 trees
248 revealed the phloem area was respectively 1.03, 1.41, 2.78, and 2.62 mm^2 and the phloem cell size was
249 respectively 89.43, 200.87, 201.07, and 181.19 μm^2 . Additionally, the #2 and #5 plants had 13,823.93
250 and 14,467.20 more phloem cells than the WT trees, respectively, whereas the #1 trees had 4491 fewer
251 phloem cells. The pith area was respectively 0.11, 0.29, 0.31, and 0.29 mm^2 in the WT, #1, #2, and #5
252 trees, and the pith cells of the transgenic trees were about 1,302–1,432 μm^2 larger than those of the WT
253 trees, but there were no obvious differences in the number of cells (Table 3). The percentage of stem
254 components was also affected by *MdBAK1* overexpression (Figure 3c). There were no obvious
255 differences in the amount of phloem among the WT, #1, and #2 trees, but the #5 trees had considerably
256 less phloem. There was also variability in the amount of xylem, pith, and other components between
257 the WT and transgenic lines. An analysis of the effects of BR (Figure 2) revealed that the BR-treated
258 2-month-old transgenic lines grew faster than the WT trees (Figure 2c). In response to a BR treatment,
259 the PH of WT, #1, #2, and #5 trees respectively increased by about 2.5, 4.5, 5.2, and 3.8 cm (Figure
260 2d).

261 **Transcriptome differences between B and WT plants.** The PSGR of 5-month-old apple trees was
262 measured after bud break, and high growth rates were detected at 30 and 120 days after bud break
263 (DABB) (Figure S11). The STs of WT and B were sampled at 0, 30, and 120 DABB, with three
264 biological replicates (WT1-1, WT1-2, WT1-3, WT2-1, WT2-2, WT2-3, WT3-1, WT3-2, WT3-3, B1-1,
265 B1-2, B1-3, B2-1, B2-2, B2-3, B3-1, B3-2, and B3-3) for an RNA sequencing analysis. A total of
266 43.43–63.27 million 150-bp paired-end reads were generated, of which approximately 78.03%–83.11%
267 were mapped to the apple genome (Table S2). There were 34,643–35,410 genes, including known and
268 new genes, in all samples (Table S2). An analysis of reproducibility indicated that the Pearson
269 correlation coefficient was high (> 0.94) (Figure S12), implying the RNA-seq data were highly robust.
270 A comparison of all samples detected 2–1,273 DEGs (Table S3).

271 A total of 1,023 DEGs were identified between WT and B (Figure 4a), including 88, 250, and 278
272 genes with upregulated expression in B1, B2, and B3, respectively, and 185, 166, and 207 genes with
273 downregulated expression in B1, B2, and B3, respectively (Figure 4a). The GO and KEGG analyses
274 were conducted to functionally characterize the DEGs (Figure 4b-c and Table S4), indicating that the
275 DEGs were commonly involved in xylem metabolism (phenylpropanoid metabolic and catabolic
276 process and lignin metabolic and catabolic process), stress responses (response to biotic stimulus,
277 antioxidant activity, carotenoid biosynthesis, biosynthesis of secondary metabolites, cyanoamino acid
278 metabolism, and glutathione metabolism), and plant hormone signal transduction (Figure 4b-c and
279 Table 4).

280 The expression levels of the lignin biosynthesis genes *MdLAC7* (*MD04G1142300*), *MdTT10*
281 (*MD07G1307400* and *MD07G1308000*), and *MdPER11* (*MD16G1052000* and *MD11G1015300*) were
282 more than 2-fold higher in B1 than in WT1. The *MdLAC7* (*MD04G1142900*) and *MdLAC11*

283 (*MD02G1145100*) expression levels were induced by 2.6- to 4-fold in B2, whereas the *MdLAC7*
284 (*MD04G1142300* and *MD04G1142600*) and *MdTT10* (*MD07G1308000*) expression levels were
285 increased by more than 2.6-fold in B3 (Figure 4b and Table 4). Several DEGs were involved in stress
286 responses (Figure 4b and Table 4). For example, genes encoding MLP-like protein 423 (*MdMLP423*;
287 *MD11G1160200*), heat shock transcription factor (*MdHSFB2A*; *MD01G1198700*), L-ascorbate
288 peroxidase (*MdAPX2*; *MD12G1125600*), phenylalanine N-monooxygenase (*MdCYP79D4*;
289 *MD11G1059700*, *MD11G1059500*, and *MD11G1059900*), delta-1-pyrroline-5-carboxylate synthetase
290 (*MD12G1150700*), chitinase (*MdCHIT1*; *MD15G1156100* and *MD02G1011100*), and
291 9-cis-epoxycarotenoid dioxygenase (*MdNCED1*; *MD10G1261000*), whose expression levels were
292 induced by about 2.5- to 12-fold in B, are involved in removing reactive oxygen . Plant hormone
293 signaling was also affected by *MdBAK1* (Figure 4c and Table 4). The *MdBAK1* (*MD15G1412700*)
294 expression level was upregulated by about 9.8-fold in B. The expression levels of the gene encoding
295 the negative ETH signal regulator EIN3-binding F-box protein (*MdEBF1*; *MD02G1030300*) was
296 repressed in B2, whereas the expression levels of the ETH-responsive transcription factor (*MdERF*)
297 genes (*MD13G1213100*, *MD10G1094700*, *MD01G1196300*, *MD02G1096500*, *MD04G1067700*,
298 *MD05G1080900*, *MD10G1094700*, and *MD15G1221100*) were inhibited in WT2 or WT3 (Table 4).
299 To test the RNA-seq results, several important DEGs were evaluated in a qRT-PCR assay (Figure S13).
300 The expression patterns of the selected genes were consistent with the RNA-seq data.

301 **Trend and Venn analyses.** For each genotype, the DEGs at three time-points were clustered into
302 eight profiles (Tables S5-S6). Profiles 0, 1, 6, and 7 were significantly overrepresented in the two
303 genotypes (Figure 5a). In B, genes related to sugar and energy metabolism (cellular carbohydrate
304 metabolic process, carbohydrate metabolic process, electron carrier activity, and sugar and sucrose
305 metabolism) were commonly enriched in the above-mentioned profiles (Figure 5b). The *alpha-amylase*
306 gene (*MdAMY1.1*; *MD08G1101700*) was grouped into profile 0, whereas *beta-glucosidase* genes
307 (*MdBGLU* genes; *MD00G1145200*, *MD12G1211500*, *MD00G1145300*, *MD05G1105800*,
308 *MD05G1105900*, *MD11G1023900*, *MD03G1068100*, *MD05G1053100*, *MD03G1068200*,
309 *MD03G1021500*, *MD13G1064200*, *MD13G1064300*, and *MD03G1098600*) were present in all of the
310 above-mentioned profiles. Genes encoding trehalose 6-phosphate phosphatase (*MdTPPI*;
311 *MD15G1365900*), 6-phosphofructokinase 3 (*MdPFK3*; *MD17G1180600*), endoglucanase 1 (*MdCEL1*;
312 *MD06G1120700*), and glucan endo-1,3-beta-glucosidase, acidic isoform GI9 (*MdPR2*;
313 *MD11G1189000*) were associated with profile 1. In contrast, genes encoding trehalose 6-phosphate
314 synthase/phosphatase (*MdTPS1*; *MD10G1270400*), *sucrose-phosphate synthase* (*MdSPS3*;
315 *MD04G1013500*), and *hexokinase* (*MdHKL3*; *MD02G1194700*) were grouped in profile 6, whereas the
316 *glucose-1-phosphate adenylyltransferase* (*MdAPS2*; *MD15G1142300*), *glucan*
317 *endo-1,3-beta-glucosidase* (*MdGNS1*; *MD12G1083900*), and
318 *phosphomannomutase/phosphoglucomutase* (*MdalgC*; *MD16G1023700*) genes belonged to profile 7
319 (Table 4). Moreover, genes related to stress responses (e.g., response to oxidative stress, response to
320 stress, and oxidoreductase activity) and protein metabolism (e.g., protein tyrosine kinase activity,
321 protein kinase activity, and cellular protein modification process) were present in the profiles of B and
322 WT (Figure 5b-c).

323 A Venn diagram was used to display the number of DEGs at three stages in WT (1,583 DEGs) and B
324 (1,754 DEGs) (Figure 6a and Tables S7-S8). An analysis of functional annotations revealed genes
325 related to hormone metabolism in B, including genes encoding cytokinin dehydrogenases (*MdCKXs*;
326 *MD14G1078600*, *MD08G1023900*, and *MD07G1026600*), activation tagged suppressor 1 (*MdPHYB*;
327 *MD13G1033900*), cytokinin synthase (*MdCYP734A1*; *MD15G1177600* and *MdIPT5*;
328 *MD13G1182800*), and cytokinin trans-hydroxylase (*MdCYP735A1*; *MD17G1076700* and
329 *MD09G1087700*) (Table 4). Additionally, genes involved in stress responses (e.g., response to
330 oxidative stress, response to water stress, and response to abiotic stimulus), metabolic pathways, fatty
331 acid elongation, biosynthesis of unsaturated fatty acid, and vitamin B6 metabolism were also identified
332 in B (Figure 6b-c). In WT, genes associated with several activities and processes were identified,
333 including the following: protein metabolism (e.g., protein phosphorylation, protein dephosphorylation,
334 and protein kinase activity), stress responses (e.g., defense response, response to oxidative stress, and
335 response to temperature stimulus), and signaling-related processes (signal transducer activity, signal
336 receptor activity, and transmembrane signaling receptor activity) (Figure 6b-c).

337 **Identification of WGCNA modules associated with target traits.** On the basis of a WGCNA, a
338 gene cluster scheme was constructed, with a power value of 5 (Figure 7a). Twelve modules, with
339 module sizes ranging from 118 to 13,104 (Figure S14 and Tables S9-S13), were identified related to
340 PH, SD, LFW, and PSGR (Figure 7b). Four modules ('brown', 'cyan', 'grey60', and 'violet') were
341 closely connected with the four above-mentioned traits ($r > 0.8$ and $p \leq 0.05$) (Figure 7b). Modules
342 'brown', 'cyan', 'brown' and 'cyan', and 'grey60' and 'violet' were highly correlated with PH, SD,
343 LFW, and PSGR, respectively. Details regarding the genes in these modules are provided in Tables
344 S10–S13. Genes related to sugar, energy, hormone, and xylem metabolic processes were commonly
345 identified in these modules. The enriched GO terms and KEGG pathways are listed in Table S14.

346 In significantly correlated modules, the gene pairs with the top-20 weight values for each trait (high
347 connectivity) were used for constructing networks (Figure S15). In the 'brown' module, genes
348 encoding the DELLA protein (*MdGAI*; *MD02G1039600*), IAA response factor 6 (*MdARF6*;
349 *MD10G1257900*), BRI1-like 1 (*MdBRL1*; *MD03G1044500*), and brassinosteroid-6-oxidase 1
350 (*MdBA13*; *MD17G1064800*) as well as genes encoding proteins related to sugar and energy [*MdAMY3*
351 (*MD09G1066000*), chlorophyllase (*MdCLH1*; *MD03G1259100*), light-harvesting complex II
352 chlorophyll a/b (*MdCAB40*; *MD10G1265300*), and ATP synthase (*MdATPG*; *MD15G1126100*)],
353 growth-regulating factor 1 (*MdGRF1*; *MD15G1216000*), and xylem-related proteins [cellulose
354 synthase-like protein E1 (*MdCSLE1*; *MD03G1028900*) and *MdLAC3* (*MD03G1056400*)] were closely
355 related to other genes (Figure S15a). Additionally, genes encoding auxilin-like protein 1 (*MdAUL1*;
356 *MD08G1028800*), glucose-induced degradation protein 8 (*MdGID8*; *MD08G1023000*), ethylene
357 (ETH) receptor 2 (*MdETR2*; *MD16G1212500*), and probable IAA efflux carrier component 1c
358 (*MdPIN1C*; *MD12G1095100*) were identified as hub genes in the 'cyan' module (Figure S15b). The

359 'grey60' module comprised 15 predicted hub genes, including hormone-related genes [*MdERF113*
360 (*MD13G1130700*), *MdARF6* (*MD05G1279200*), *MdGAIPB* (*MD16G1023300*), *MdSWEET15*
361 (*MD13G1124300*), *MdEDL16* (*MD13G1175900*), *MdARR11* (*MD16G1108400*), and *MdBSK*
362 (*MD12G1156600*)], sugar and energy metabolism-related genes [*glucose-6-phosphate isomerase*
363 (*MdPGIC1*; *MD08G1034600*), *sucrose synthase* (*MdSS*; *MD02G1100500*), *MdPFK3*
364 (*MD17G1180800*), *beta-mannan synthase* (*MdCSLA9*; *MD12G1016200*), *beta-amylase* (*MdBAM1*;
365 *MD13G1226400*), and *photosystem I subunit XI* (*MdPSAL*; *MD12G1260300*)], and xylem
366 metabolism-related genes [*MdLAC17* (*MD12G1144300*) and *MdCESA7* (*MD02G1005600*)] (Figure
367 S15c). The 'violet' module consisted of eight hub genes, including *MdARR12* (*MD15G1037400*),
368 *MdBKII* (*MD15G1084100*), an IAA-induced protein gene (*MdAUX28*; *MD10G1192900*), *MdARF1*
369 (*MD08G1247700*), *MdGAI* (*MD09G1264800*), *MdTPS1* (*MD03G1250300*), *MdIRX12*
370 (*MD07G1213300*), and the cell division cycle 20-like protein 1 gene (*MdFZR3*; *MD01G1136000*)
371 (Figure S15d).

372 **Effect of *MdBAK1* overexpression on endogenous hormone and carbohydrate contents.** The
373 RNA-seq analysis suggested that BR, CTK, and carbohydrates may be crucial for apple growth and
374 development. Therefore, their contents were measured in the WT and transgenic trees (Figure S16). In
375 WT trees, endogenous BR levels changed by about 3.3 ng/g over five time-points. However, among the
376 #1, #2, and #5 trees, the BR content first sharply increased, peaking (about 16–20 ng/g) at 30 DABB,
377 and then decreased, reaching its lowest level (about 6–10 ng/g) at 180 DABB. Overall, the BR level
378 was higher in B than in WT trees from 30 to 90 DABB, whereas the opposite pattern was observed at
379 180 DABB. Similarly, the extent of the change in CTK levels was smaller for WT trees than for the
380 transgenic trees (about 4, 14, 9, and 7 ng/g for the WT, #1, #2, and #5 trees, respectively).

381 The greatest difference in starch levels between the WT and transgenic trees over the analyzed
382 time-period was a 3.6- to 3.8-fold higher level in transgenic trees. Starch contents were generally
383 higher in the transgenic lines than in the WT trees from 0 to 90 DABB, but the opposite pattern was
384 detected from 120 to 180 DABB. The sucrose level in the transgenic lines increased by about 7–9 mg/g
385 from 0 to 30 DABB, whereas it only changed by about 3 mg/g in the WT trees. At the other time-points
386 (except for 120 DABB), there were no differences in the sucrose concentration between the WT trees
387 and transgenic lines. The trehalose content in #1, #2, and #5 trees exhibited an obvious downward trend
388 from 0 to 180 DABB, but it changed only slightly in the WT trees. Regarding the glucose levels in the
389 WT, #1, #2, and #5 trees, they respectively increased by about 3, 6, 8, and 6 mg/g from 0 to 30 DABB,
390 decreased by about 2, 9, 10, and 9 mg/g from 30 to 90 DABB, increased by 1, 9, 11, and 10 mg/g from
391 90 to 120 DABB, and then decreased by about 2, 8, 8, and 9 mg/g from 120 to 180 DABB. Among all
392 plants, there was no significant difference in the sorbitol level at most time-points. In contrast, the
393 fructose concentration in the transgenic trees was 5–14 mg/g higher than that in the WT trees. The

394 changes to the total soluble sugar content over the study period were more obvious in the
395 *MdBAK1*-overexpressing lines than in the WT control.

396 **DISCUSSION**

397 ***MdBAK1* positively influences plant growth through involving in BR signal transduction.** The
398 *AtBAK1* gene encodes an essential BR signal receptor.²⁴ Additionally, *AtBAK1* and *MdBAK1* contain
399 similar conserved domains (Figure S1a). Like *AtBAK1*, *MdBAK1* is localized in the cell membrane
400 (Figure S5).²⁵ A phylogenetic analysis revealed that *MdBAK1* is most closely related to *PaBAK1*
401 (Figure S1b). Moreover, *MdBAK1* expression was induced by a BR treatment (Figure S2b–d). These
402 results indicate that, like *AtBAK1*, *MdBAK1* may affect BR signal transduction.

403 Previous studies proved that high BR concentrations inhibit root growth, whereas *A. thaliana*, *Oryza*
404 *sativa*, and *Zea mays bri1* mutants exhibit abnormal BR signaling are insensitive to exogenous BR.² In
405 the current study, the transgenic *A. thaliana* plants were more sensitive to BR than the WT plants
406 (Figure 2a-b). The application of exogenous BR accelerated the growth of transgenic apple trees more
407 than WT trees (Figure 2c-d). These results imply that *MdBAK1* expression may be induced by BR to
408 regulate plant growth.

409 The BR synthesis and signal transduction genes help control plant growth.² However, there is a
410 relative lack of information regarding the regulatory role of *MdBAK1* related to plant growth and
411 development. In this study, the overexpression of *MdBAK1* in *A. thaliana* and apple plants resulted in
412 increased biomass (Figures S8–10). Additionally, the stem cell length increased following *MdBAK1*
413 overexpression (Figures 1a-b and 3a and Table 2), which may lead to stem elongation. Moreover, the
414 stem area as well as cell size and number were greater in transgenic plants than in WT plants (Figures

415 1c and 3b and Tables 1-2). These results indicate that *MdBAK1* promotes plant growth.

416 **Roles of DEGs between WT and transgenic apple trees in ETH signaling, xylem metabolism,**
417 **and stress responses.** A comparison of WT and transgenic apple trees revealed DEGs related to BR
418 signaling, ETH signaling, xylem metabolism, and stress responses (Figure 4 and Table 4). As a BR
419 receptor, *MdBAK1* should be closely related to other BR signaling components. This close relationship
420 was verified by the identified BR signaling-related DEGs (Figure 4c and Table 4) and the sensitivity of
421 the transgenic plants to exogenous BR (Figure 2). The overexpression of *MdBAK1* enhanced ETH
422 signal transduction by downregulating and upregulating the *MdEBF1* and *MdERF* expression levels,
423 respectively (Figure 4c and Table 4). In *A. thaliana*, BR, IAA, and CTK treatments commonly promote
424 ETH production.²⁶ In rice, an upstream component of the BR signaling pathway may activate ETH
425 signaling.²⁷ In banana, *BZR1/2* regulate ETH biosynthesis during the fruit ripening stage.²⁸ Previous
426 studies confirmed that ETH positively regulates cell and stem elongation.²⁹ In rice, ETH can promote
427 internode elongation by activating GA synthesis.³⁰ In transgenic tomato plants, the overexpression of
428 the grape ETH synthase gene (*VvACS*) alters shoot and root formation.³¹ These findings suggest that
429 *MdBAK1* may promote apple stem elongation through the ETH signal pathway, but this possibility is
430 supposed to be verified experimentally.

431 Earlier studies concluded that BR genes are crucial for lignin formation.³ In the current study, the
432 expression levels of lignin biosynthesis genes (*MdLAC*, *MdTT10*, and *MdPER* genes) were induced by
433 *MdBAK1* (Table 4), and the overexpression of *MdBAK1* in *A. thaliana* and apple plants generally
434 promoted xylem growth in the stem (Figures 1 and 3 and Tables 1-2). Thus, similar to other BR genes,
435 *MdBAK1* is associated with increased xylem production. The *BAK1* gene is reportedly responsive to

436 biotic and abiotic stresses.¹⁰ We observed that stress-related genes (e.g., *MdMLP423*, *MdHSFB2A*, and
437 *MdAPX2*) exhibited upregulated expression in transgenic apple samples (Table 4). This suggests
438 *MdBAK1*, like *BAK1* in other species, may contribute to stress responses through the above-mentioned
439 genes.

440 **Genes that are differentially expressed over time participate in carbohydrate and CTK**
441 **metabolism.** To fully explore the biological functions of *MdBAK1*, profile and Venn analyses were
442 performed at three different time-points. Our profile analysis indicated that starch-, sucrose-, trehalose-,
443 glucose- and fructose-related genes were enriched in B (Figure 5b-c). Moreover, the contents of most
444 of the analyzed carbohydrates in B changed substantially over time (Figure S16). Energy production is
445 closely linked to sugar metabolism, and energy-related genes (e.g., *MdKKL3* and *MdalgC*) were also
446 classified into specific profiles in B. Brassinosteroids affect sugar and energy metabolism, with many
447 BR genes (e.g., *CPD*, *DWF*, and *BZR1*) reportedly involved in this process.³² Therefore, *MdBAK1* may
448 contribute to carbohydrate and energy metabolism during apple tree growth and development.

449 Our Venn analysis indicated that compared with WT trees, hormone metabolism was enriched in B
450 trees (Figure 6b-c and Table 4). Additionally, BR and CTK changed more sharply in the transgenic
451 lines at various time-points (Figure S16). Moreover, BR and CTK, which are closely associated, are
452 two of the most important plant hormones² that commonly regulate root growth, chloroplast
453 development, stem growth, and drought tolerance.³³ Accordingly, we speculate that apple tree growth
454 may be affected by *MdBAK1*-mediated crosstalk between BR and CTK.

455 **The hub genes in the WGCNA module control sugar, hormone and xylem metabolism as well**
456 **as cell growth.** Our WGCNA results indicated that sugar and energy metabolism, hormone
457 metabolism, xylem metabolism, and cell growth are significantly correlated with target traits, which is
458 consistent with the findings of our DEG analysis (Figures 7 and S14 and Tables 3 and S14).
459 Brassinosteroids share close relationships with CTK and ETH as well as with GA and IAA. Previous
460 studies proved that BR and GA can function cooperatively to regulate PH and tillering.³⁴ Additionally,
461 AtBZR1/2 control the transcription of GA biosynthesis genes³⁵ and can interact with DELLA³⁶.
462 Moreover, BR also participates in the polar transport of IAA,³⁷ and BIN2 can decrease ARF
463 activities.³⁸ In the current study, BR genes (*MdBA13*, *MdBRL1*, *MdBSK*, and *MdBK11*), GA genes
464 (*MdGAI* and *MdSWEET*), IAA genes (*MdPINIC* and *MdARF6*), ETH genes (*MdETR2* and
465 *MdERF113*), and a CTK gene (*MdARR11*) were highly correlated with other genes in significant
466 modules, indicating *MdBAK1* likely affects the crosstalk between BR and other hormones. Cell growth
467 genes were also identified as hub genes (Figure S15). Considering the positive effects of BR on cell
468 growth (Figures 1 and 3 and Tables 1-3), these findings indicate these cell-related genes may be
469 involved in *MdBAK1*-mediated stem cell growth. Moreover, some of these hub genes in other species
470 are involved in stem and leaf growth.³⁹ For example, *MdGAI*-overexpressing transgenic tomato plants
471 are shorter than normal, and exhibit dwarfism phenotypes.⁴⁰ Additionally, *MdPIN1* is involved in the
472 regulation of apple tree height.⁴¹ Therefore, the above-mentioned hub genes should be examined in
473 greater detail in future studies regarding *MdBAK1*-mediated apple tree growth. Furthermore, the
474 interesting candidate genes will need to be verified in future investigations.

475 Overall, the molecular mechanism underlying *MdBAK1* functions was clarified through
476 morphological and RNA-seq analyses. We also proposed a model for *MdBAK1*-mediated apple tree

477 growth, involving hormone, xylem, and sugar and energy metabolic activities (Figure 8). Specifically,
478 *MdBAK1* overexpression activates the BR signal, and enhances xylem production by upregulating
479 *MdLAC*, *MdTT10*, and *MdPER11* expression levels. The ETH signal is also activated via altered
480 *MdEBF1* and *MdERF* expression levels. Additionally, the *MdBAK1*-overexpressing transgenic lines are
481 likely insensitive to biotic and abiotic stress. Sugar and energy metabolism (i.e., starch, glucose,
482 sucrose, trehalose, fructose, and TCA) is strongly affected by *MdBAK1* during growth. A Venn
483 analysis confirmed that *MdCKX-MdIPT-MdCYP735A1* and *MdPHYB-MdCYP734A1* respectively alter
484 CTK and BR metabolism in transgenic apple trees during the growing season. A WGCNA revealed
485 that genes related to sugar and energy (e.g., *MdAMY3*, *MdCLH1*, and *MdCAB40*), BR (*MdBAl3*,
486 *MdBRL1*, *MdBSK*, and *MdBK11*), GA (*MdGAI*), IAA (*MdPINIC* and *MdARF6*), ETH (*MdETR2* and
487 *MdERF113*), xylem (*MdCSLE1*, *MdLAC3/17*, *MdCESA7*, and *MdIRX12*), and cell growth (*MdGRF1*,
488 *MdAUL1*, and *MdFZR3*) are pivotal targets of *MdBAK1*. All of these factors commonly regulate apple
489 tree growth.

490 The results of this study provide new information regarding the *BAK1* gene, and confirm the
491 connections among *BAK1*, xylem metabolism, and the ETH signal. However, *MdBAK1* must still be
492 further characterized. For example, it remains unclear why *MdBAK1* overexpression leads to
493 fluctuations in hormone, sugar, and energy metabolic activities, and how these elements positively
494 regulate apple tree growth. These phenomena may be complicated in perennial fruit trees, and will need
495 to be clarified in future studies. Nevertheless, the data presented herein will help to completely
496 characterize the molecular mechanism regulating *MdBAK1*-mediated growth.

497 **AUTHOR INFORMATION**

498 **Corresponding Authors**

499 *;E-mail: hanmy@nwsuaf.edu.cn; Tel: 86-029- 87082543.

500 * E-mail: anna206@nwsuaf.edu.cn; Tel: 86-029- 87082543.

501 **ORCID**

502 Na An: 0000-0002-7855-4447

503 **Funding**

504 Authors Na An and XiaolinRen received funding from the Natural Science Foundation of China

505 (31672101 and 31872937), the Screening and Interaction Molecular Mechanism of Apple Stock and

506 Scion Combinations (K3380217027), the National Apple Industry Technology System of the

507 Agriculture Ministry of China (CARS-28), the Ecological Adaptability Selection of Apple Superior

508 Stock and Scion Combinations in the Loess Plateau (A2990215082), the Science and Technology

509 Innovative Engineering Project in Shaanxi Province of China (2015NY114, 2016KTZDNY01-10, and

510 2017NY0055), the Yangling Subsidiary Center Project of the National Apple Improvement Center

511 (Z100021809), the Innovation Project of Science and Technology of Shaanxi Province

512 (2016TZC-N-11-6), the Key Research Project of Shaanxi Province (2017ZDXM-NY-019), and the

513 Tang Scholarship of the Cyrus Tang Foundation and Northwest A & F University (2018NY-08).

514 **Notes**

515 The authors declare no competing financial interests.

516 **ACKNOWLEDGMENTS**

517 Na An and Xiaolin Ren supervised this study. Liwei Zheng, Yingli Yang, Cai Gao, Juanjuan Ma, Dong

518 Zhang, Caiping Zhao, Libo Xing, Mingyu Han, and Na An prepared the samples. Liwei Zheng and Na

519 An analyzed the transcriptomic data and performed all experiments. Liwei Zheng, Kamran Shah and
520 Na An wrote and revised the manuscript. We thank Liwen Bianji, Edanz Editing China
521 (www.liwenbianji.cn/ac) for editing the English text of a draft of this manuscript.

522

523 **ABBREVIATIONS USED**

524 BRs, Brassinosteroids; WT, wild-type; RNA-seq, RNA-sequencing; WGCNA, weighted gene
525 co-expression network analysis; ST, shoot tip; YX, xylem of young stem; YP, phloem of young stem;
526 MX, xylem of mature stem; MP, phloem of mature stem; JL, juvenile leaves; ML, mature leaves; R,
527 new roots; M.9-T337, Malling 9-T337; MS, Murashige and Skoog; BL, brassinolide; GFP, green
528 fluorescent protein; Col-0, Columbia; PH, Plant height; CTK, cytokinin; HPLC-MS, high-performance
529 liquid chromatography-mass spectrometry; DEGs, Differentially expressed genes; STEM, Short
530 Time-series Expression Miner; SD, stem diameter; LFW, leaf fresh weight; PSGR, primary shoot
531 growth rate; GO, gene ontology; KEGG, Kyoto Encyclopedia of Genes and Genomes; SPSS, Statistical
532 Product and Service Solutions

533 **Supplementary materials**

534 **Table S1. Details regarding the primers used in this study**

535 *MdBAK1* (MD15G1412700)-pCAMBIA1302, *MdBAK1* (MD15G1412700)-pCAMBIA1301, and
536 *MdBAK1* (MD15G1412700)-pCAMBIA2300 were respectively constructed as the subcellular
537 localization vector as well as the plant-overexpression vectors for *Arabidopsis thaliana* and apple. The
538 *TUB* and *EF-1 α* genes were used to standardize the gene expression levels in *A. thaliana* and apple.

539 **Table S2. Transcriptome sequencing and assembly statistics**

540 **Table S3. Statistical analysis of DEGs between WT and B plants**

541 **Table S4. Details regarding the DEGs between WT and B plants**

542 **Table S5. Details regarding the DEGs used for the trend analysis in WT plants**

543 **Table S6. Details regarding the DEGs used for the trend analysis in B plants**

544 **Table S7. Details regarding the DEGs used for the Venn analysis in WT plants**

545 **Table S8. Details regarding the DEGs used for the Venn analysis in B plants**

546 **Table S9. Number of genes in each WGCNA module**

547 **Table S10. Genes in the ‘brown’ module**

548 **Table S11. Genes in the ‘cyan’ module**

549 **Table S12. Genes in the ‘grey60’ module**

550 **Table S13. Genes in the ‘violet’ module**

551 **Table S14. Distribution of functional categories in significant WGCNA modules according to GO**
552 **and KEGG pathway databases**

553 **Figure S1.** Sequence alignment and phylogenetic analysis of BAK1 in various plant species.

554 (a) Alignment of *Malus domestica* (Md), *Populus tomentosa* (Pt), *Prunus avium* (Pa), *Theobroma*

555 *cacao* (Tc), *Helianthus annuus* (Ha), *Gossypium hirsutum* (Gh), *Jatropha curcas* (Jc), *Chrysanthemum*
556 *boreale* (Cb), *Hevea brasiliensis* (Hb), *Morus notabilis* (Mn), *Cajanus cajan* (Cc), *Arachis ipaensis*
557 (Ai), *Arachis duranensis* (Ad), *Glycine soja* (Gs), *Arabidopsis lyrata* subsp. *lyrata* (Al), *Arabidopsis*
558 *thaliana* (At), *Solanum lycopersicum* (Sl), *Gossypium arboreum* (Ga), and *Sesamum indicum* (Si)
559 BAK1 proteins. The signal peptide, leucine-rich zippers, LRR1, LRR2, LRR3, LRR4, LRR5,
560 proline-rich region, transmembrane domain, and kinase domain are respectively marked by 1–10.
561 Conserved function-related sites (D122, K317, C408, D416, D434, and T455) are indicated by arrows.

562 (b) Phylogenetic tree presenting the evolutionary relationships of BAK1 proteins in various plant
563 species.

564 **Figure S2.** Expression pattern of *MdBAK1* in apple.

565 (a) *MdBAK1* transcription level in various tissues of 1-year-old M.9-T337. (b) Rapid response of
566 *MdBAK1* to an exogenous BR treatment. (c) *MdBAK1* expression level in M.9-T337 at 0, 14, 28, 42,
567 and 56 days after a BR treatment. (d) *MdBAK1* transcription pattern in *Malus prunifolia* at 0, 7, 14, 28,
568 and 42 days after a BR treatment.

569 **Figure S3.** Endogenous BR level in shoot tips after a BR treatment.

570 The BR content was detected according to an HPLC-MS technique. Values are presented as the mean \pm
571 standard error of three replicates.

572 **Figure S4.** Effect of BR on *Malus prunifolia* growth.

573 (a) Phenotype of control and treated *Malus prunifolia* at 42 days after a BR treatment. (b) Plant height,
574 average internode length, number of nodes, shoot fresh weight, leaf fresh weight, and leaf area of
575 control and BR-treated apple trees. Values are presented as the mean \pm standard error of nine
576 replicates.

577 **Figure S5.** Subcellular localization of MdBAK1.

578 Confocal images of transiently transformed tobacco epidermal cells with the green fluorescent protein
579 (GFP), MdBAK1-GFP, or mock infection liquid.

580 **Figure S6.** Molecular analysis of *MdBAK1*-overexpressing transgenic *Arabidopsis thaliana*.

581 (a) Schematic diagram of the T-DNA region of the binary pCAMBIA1301 vector for *A. thaliana*
582 transformation. LB: left T-DNA border, RB: right T-DNA border, Ter: terminator, CaMV35S:
583 Cauliflower mosaic virus 35S promoter, *HYG*: hygromycin phosphotransferase gene, and GUS:
584 β -glucuronidase. (b) Results of a PCR analysis of the transgenic and WT *A. thaliana*. M: marker, WT:
585 wild-type, and 1–7: different transgenic lines. (c) Results of a qRT-PCR analysis of *MdBAK1*
586 expression levels in transgenic and WT lines.

587 **Figure S7.** Molecular analysis of *MdBAK1*-overexpressing transgenic apple.

588 (a) Structure of the 35S:*MdBAK1* construct for the expression of *MdBAK1*. LB: left T-DNA border,
589 RB: right T-DNA border, Ter: terminator, CaMV35S: Cauliflower mosaic virus 35S promoter, *NPTII*:
590 neomycin phosphotransferase gene, and GFP: protein tag used for a western blot. (b) Results of a PCR
591 analysis of the transgenic and WT apple. M: marker, WT: wild-type, 1 to 6: different transgenic lines,
592 and P: plasmid. (c) Western blot analysis of the MdBAK1 levels in the leaves of WT and transgenic
593 lines. (d) Analysis of *MdBAK1* expression among the transgenic and WT apple.

594 **Figure S8.** Analysis of phenotype and physiological data of wild-type and three independent
595 *MdBAK1*-overexpressing transgenic *Arabidopsis thaliana* plants.

596 (a) Phenotypes of WT and *MdBAK1*-overexpressing 21-day-old seedlings. (b) Phenotypes of
597 60-day-old WT and *MdBAK1*-overexpressing *A. thaliana*. (c) Plant height, average internode length,
598 number of nodes, stem diameter, shoot fresh weight, and seedling fresh weight of 60-day-old plants.

599 Values are presented as the mean \pm standard error of nine replicates.

600 **Figure S9.** Phenotypes of WT and *MdBAK1*-overexpressing transgenic plants cultured on MS medium.

601 (a) One-month-old seedlings cultured on MS medium. (b) Statistical analysis of whole seedling weight
602 of WT and *MdBAK1*-overexpressing transgenic apple lines. Values are presented as the mean \pm
603 standard error of nine replicates.

604 **Figure S10.** Analysis of phenotype and physiological data of WT and three independent
605 *MdBAK1*-overexpressing transgenic apple trees.

606 (a and c) Phenotypes of 2-month-old and 5-month-old WT, MdBAK1-OX#1, MdBAK1-OX#2, and
607 MdBAK1-OX#5 trees. (b and d) Plant height, stem diameter, average internode length, stem fresh
608 weight, stem dry weight, leaf fresh weight, leaf dry weight, and leaf area of 2-month-old and
609 5-month-old WT and transgenic apple trees. Three biological replicates (three trees per biological
610 replicate) and three technical replicates of the WT and transgenic lines were analyzed. * significant
611 differences at the 0.05 level.

612 **Figure S11.** Primary shoot growth rate of WT and *MdBAK1*-overexpressing transgenic trees grown in
613 the greenhouse after bud break.

614 Primary shoot growth rate per day for WT, MdBAK1-OX#1, MdBAK1-OX#2, and MdBAK1-OX#5
615 trees. Values are presented as the mean \pm standard error of nine replicates.

616 **Figure S12.** Transcriptome relationships among three biological replicates.

617 **Figure S13.** Validation of crucial DEGs in WT and B via quantitative real-time PCR.

618 All gene expression levels were normalized relative to expression level in the non-treated WT control.

619 **Figure S14.** Gene expression patterns.

620 A heatmap was used to visualize the expression patterns of 12 modules (dark green, light green,

621 yellow, dark turquoise, brown, black, light yellow, steel blue, grey60, violet, cyan, and orange). The
622 color bar indicates the gene expression levels [low (green) to high (red)].

623 **Figure S15.** Cytoscape representation of the network relationships with an edge weight ≥ 0.10 in
624 significant modules.

625 (a to d) Network relationships of the 'brown', 'cyan', 'grey60', and 'violet' modules, respectively. The
626 edge weight of the genes, which is indicated with a color-coded scale, is positively related to the size of
627 the circle. Member gene IDs and names are provided.

628 **Figure S16.** Changes to hormone and sugar contents across five time-points.

629 Brassinosteroid, cytokinin, starch, sucrose, trehalose, glucose, sorbitol, fructose, and total soluble sugar
630 contents were determined at 0, 30, 90, 120, and 180 DABB for the WT, MdBAK1-OX#1,
631 MdBAK1-OX#2, and MdBAK1-OX#5 plants. Three biological replicates (three trees per replicate) and
632 three technical replicates of the WT and transgenic lines were analyzed. * significant differences at the
633 0.05 level.

634 **Table legends**

635 **Table 1. Analysis of *Arabidopsis thaliana* stem vascular bundle structures**

636 **Table 2. Analysis of average cell lengths in longitudinal stem sections**

637 Different letters indicate significant differences at the 0.05 level. Three replicates (three trees per
638 replicate) of the WT and transgenic lines were analyzed.

639 **Table 3. Structural analysis of stem cross sections**

640 Different letters indicate significant differences at the 0.05 level. Three replicates (three trees per
641 replicate) of the WT and transgenic lines were analyzed.

642 **Table 4. Differentially expressed genes involved in important processes in response to MdbAK1**

643 **Figure legends**

644 **Figure 1.** Anatomical analysis of the *Arabidopsis thaliana* stem.

645 (a) Partial longitudinal sections. (b) Pith cell length of WT, MdbAK1-OX#1, MdbAK1-OX#3, and
646 MdbAK1-OX#4. (c) Stem cross-section. (d) Proportion of stem cross-section represented by the
647 xylem, phloem, pith, and other components (includes the epidermis, cortex, and interfascicular
648 cambium). 1: pith; 2: xylem; 3: phloem; 4: cortex. Values are presented as the mean \pm standard error of
649 three replicates.

650 **Figure 2.** Analysis of the BR sensitivity of WT and transgenic lines.

651 (a) Phenotype of 7-day-old BR-treated seedlings grown under light. (b) Root length of WT and
652 transgenic *Arabidopsis thaliana* at 7 days after a BR treatment. Values are presented as the mean \pm
653 standard error of nine replicates. (c) Phenotype of WT and transgenic apple trees treated with BR. (d)
654 Plant height of WT and transgenic apple trees treated with BR. Three biological replicates (three trees

655 per replicate) and three technical replicates were analyzed. Different letters indicate significant
656 differences at the 0.05 level.

657 **Figure 3.** Anatomical analysis of the apple tree stem.

658 (a) Longitudinal stem section. (b) Stem cross-section. (c) Proportion of the stem cross-section
659 represented by the xylem, phloem, pith, and other components (includes the epidermis, cortex, and
660 interfascicular cambium). 1: cortex; 2: phloem; 3: xylem; 4: pith. Three biological replicates (three
661 trees per replicate) of the WT and transgenic lines were analyzed.

662 **Figure 4.** Analysis of the functional enrichment of the DEGs between WT and B plants.

663 (a) Venn diagrams of all genes exhibiting up- or downregulated expression between WT and B plants.
664 (b) Results of the GO enrichment analysis of the DEGs between WT and B plants. (c) Results of the
665 KEGG pathway enrichment analysis of the DEGs between WT and B plants.

666 **Figure 5.** Gene expression patterns and enrichment of GO terms and KEGG pathways across three
667 time-points in WT and B plants.

668 (a) Gene expression patterns at three time-points in WT and B plants predicted with STEM software.
669 The number of genes and *p*-values for each pattern are indicated in the frame. (b) Results of the GO
670 enrichment analysis of important processes in WT and B plants. (c) Results of the KEGG pathway
671 enrichment analysis of important processes in WT and B plants. The *p*-value was used to indicate the
672 significance of the most represented GO and KEGG Slim terms. Significant *p*-values are indicated in
673 red, whereas non-significant *p*-values are indicated in dark gray.

674 **Figure 6.** Venn analysis of DEGs over time in WT and B.

675 (a) Number of DEGs in the WT and B plants. (b) Clusters of annotated GO terms for the DEGs in the
676 WT and B plants. (c) Results of the KEGG pathway enrichment analysis of the DEGs in the WT and B

677 plants. The significance of the most represented terms is indicated by a p -value. Significant p -values are
678 indicated in red, whereas non-significant p -values are indicated in dark gray.

679 **Figure 7.** Weighted gene co-expression network analysis (WGCNA) of genes identified in the WT and
680 B plants over three developmental stages.

681 (a) Twelve modules of co-expressed genes are shown in a hierarchical cluster tree. A major tree branch
682 represents a module. Modules in designated colors are presented in the lower panel. (b) Module-trait
683 relationships. The 12 modules are provided in the left panel. The module-trait correlation, from -1
684 (green) to 1 (red), is indicated with the color scale on the right. Each column presents the experimental
685 traits, and their association with each module is represented by a correlation coefficient and a p -value
686 in parentheses.

687 **Figure 8.** Proposed model for the *MdBAK1* overexpression-mediated regulation of apple tree growth.

688 A comparative analysis revealed that BR signaling, xylem production, ETH signaling, and stress
689 responses are activated during shoot growth, and are respectively indicated with orange, black, blue
690 and carmine curves. Arrows (positive regulation) or blocked arrows (negative regulation) represent
691 crucial metabolic steps. The expression levels of genes in red or blue are respectively upregulated or
692 downregulated in B. The trend and Venn analyses indicated that sugar and energy and hormone
693 metabolic activities are enriched over time. Crucial metabolic pathways and genes based on a WGCNA
694 are indicated.

695

696

697 **References**

698 (1) Gou, X.; Yin, H.; He, K.; Du J; Yi, J.; Xu, S.; Lin, H.; Clouse, S. D.; Li, J. Genetic evidence for
699 an indispensable role of somatic embryogenesis receptor kinases in brassinosteroid signaling. *PLoS*
700 *Genet.* **2012**, 8 (1), e1002452.

701 (2) Clouse, S. D.; Langford, M.; McMorris, T. C. A brassinosteroid-insensitive mutant in
702 *Arabidopsis thaliana* exhibits multiple defects in growth and development. *Plant Physiol.* **1996**, 111 (3),
703 671-8.

704 (3) Zheng, L.; Zhao, C.; Mao, J.; Song, C.; Ma, J.; Zhang, D.; Han, M.; An, N. Genome-wide
705 identification and expression analysis of brassinosteroid biosynthesis and metabolism genes regulating
706 apple tree shoot and lateral root growth. *J. Plant Physiol.* **2018**, 231, 68-85.

707 (4) Yang, C. J.; Zhang, C.; Lu, Y. N.; Jin, J. Q.; Wang, X. L. The mechanisms of brassinosteroids'
708 action: from signal transduction to plant development. *Mol. Plant* **2011**, 4 (4), 588-600.

709 (5) Wang, D.; Yang, C.; Wang, H.; Wu, Z.; Jiang, J.; Liu, J.; He, Z.; Chang, F.; Ma, H.; Wang, X.
710 BKI1 Regulates Plant Architecture through Coordinated Inhibition of the Brassinosteroid and
711 ERECTA Signaling Pathways in *Arabidopsis*. *Mol. Plant* **2017**, 10 (2), 297-308.

712 (6) Sanchez-Rodriguez, C.; Ketelaar, K.; Schneider, R.; Villalobos, J. A.; Somerville, C. R.; Persson,
713 S.; Wallace, I. S. BRASSINOSTEROID INSENSITIVE2 negatively regulates cellulose synthesis in
714 *Arabidopsis* by phosphorylating cellulose synthase 1. *Proc Natl Acad Sci U S A* **2017**, 114 (13),
715 3533-3538.

716 (7) Qiao, S.; Sun, S.; Wang, L.; Wu, Z.; Li, C.; Li, X.; Wang, T.; Leng, L.; Tian, W.; Lu, T.; Wang,
717 X. The RLA1/SMOS1 Transcription Factor Functions with OsBZR1 to Regulate Brassinosteroid
718 Signaling and Rice Architecture. *Plant Cell* **2017**, 29 (2), 292-309.

719 (8) Nam, K. H.; Li, J. BRI1/BAK1, a receptor kinase pair mediating brassinosteroid signaling. *Cell*
720 **2002**, 110 (2), 203-12.

721 (9) Chinchilla, D.; Zipfel, C.; Robatzek, S.; Kemmerling, B.; Nurnberger, T.; Jones, J. D.; Felix, G.;
722 Boller, T. A flagellin-induced complex of the receptor FLS2 and BAK1 initiates plant defence. *Nature*
723 **2007**, 448 (7152), 497-500.

724 (10) Shan, L.; He, P.; Li, J.; Heese, A.; Peck, S. C.; Nurnberger, T.; Martin, G. B.; Sheen, J. Bacterial
725 effectors target the common signaling partner BAK1 to disrupt multiple MAMP receptor-signaling
726 complexes and impede plant immunity. *Cell Host Microbe* **2008**, 4 (1), 17-27.

727 (11) Wang, H.; Mei, W.; Qin, Y.; Zhu, Y. 1-Aminocyclopropane-1-carboxylic acid synthase 2 is
728 phosphorylated by calcium-dependent protein kinase 1 during cotton fiber elongation. *Acta Biochim*
729 *Biophys Sin (Shanghai)* **2011**, 43 (8), 654-61.

730 (12) Lu, D.; Wu, S.; Gao, X.; Zhang, Y.; Shan, L.; He, P. A receptor-like cytoplasmic kinase, BIK1,
731 associates with a flagellin receptor complex to initiate plant innate immunity. *Proc Natl Acad Sci U S A*
732 **2010**, 107 (1), 496-501.

733 (13) Qian, M.; Zhang, Y.; Yan, X.; Han, M.; Li, J.; Li, F.; Li, F.; Zhang, D.; Zhao, C. Identification
734 and Expression Analysis of Polygalacturonase Family Members during Peach Fruit Softening. *Int. J.*
735 *Mol. Sci.* **2016**, 17 (11).

736 (14) Clough, S. J.; Bent, A. F. Floral dip: a simplified method for *Agrobacterium*-mediated
737 transformation of *Arabidopsis thaliana*. *Plant J.* **1998**, 16 (6), 735-43.

- 738 (15) Cheng, S.; Xie, X.; Xu, Y.; Zhang, C.; Wang, X.; Zhang, J.; Wang, Y. Genetic transformation of
739 a fruit-specific, highly expressed stilbene synthase gene from Chinese wild *Vitis quinquangularis*.
740 *Planta* **2016**, 243 (4), 1041-53.
- 741 (16) Rosa, M.; Hilal, M.; Gonzalez, J. A.; Prado, F. E. Low-temperature effect on enzyme activities
742 involved in sucrose-starch partitioning in salt-stressed and salt-acclimated cotyledons of quinoa
743 (*Chenopodium quinoa* Willd.) seedlings. *Plant Physiol Biochem* **2009**, 47 (4), 300-7.
- 744 (17) Gambino, G.; Perrone, I.; Gribaudo, I. A Rapid and effective method for RNA extraction from
745 different tissues of grapevine and other woody plants. *Phytochem Anal* **2008**, 19 (6), 520-5.
- 746 (18) Langmead, B.; Trapnell, C.; Pop, M.; Salzberg, S. L. Ultrafast and memory-efficient alignment
747 of short DNA sequences to the human genome. *Genome Biol* **2009**, 10 (3), R25.
- 748 (19) Daccord, N.; Celton, J. M.; Linsmith, G.; Becker, C.; Choisne, N.; Schijlen, E.; van de Geest, H.;
749 Bianco, L.; Micheletti, D.; Velasco, R.; Di Pierro, E. A.; Gouzy, J.; Rees, D.; Guerif, P.; Muranty, H.;
750 Durel, C. E.; Laurens, F.; Lespinasse, Y.; Gaillard, S.; Aubourg, S.; Quesneville, H.; Weigel, D.; van
751 de Weg, E.; Troggio, M.; Bucher, E. High-quality de novo assembly of the apple genome and
752 methylome dynamics of early fruit development. *Nat. Genet.* **2017**, 49 (7), 1099-1106.
- 753 (20) Kim, D.; Pertea, G.; Trapnell, C.; Pimentel, H.; Kelley, R.; Salzberg, S. L. TopHat2: accurate
754 alignment of transcriptomes in the presence of insertions, deletions and gene fusions. *Genome Biol*
755 **2013**, 14 (4), R36.
- 756 (21) Mortazavi, A.; Williams, B. A.; McCue, K.; Schaeffer, L.; Wold, B. Mapping and quantifying
757 mammalian transcriptomes by RNA-Seq. *Nat. Methods* **2008**, 5 (7), 621-8.
- 758 (22) Langfelder, P.; Horvath, S. WGCNA: an R package for weighted correlation network analysis.
759 *BMC Bioinformatics* **2008**, 9, 559.

760 (23) Shannon, P.; Markiel, A.; Ozier, O.; Baliga, N. S.; Wang, J. T.; Ramage, D.; Amin, N.;
761 Schwikowski, B.; Ideker, T. Cytoscape: a software environment for integrated models of biomolecular
762 interaction networks. *Genome Res.* **2003**, 13 (11), 2498-504.

763 (24) Baudino, S.; Hansen, S.; Brettschneider, R.; Hecht, V. F.; Dresselhaus, T.; Lorz, H.; Dumas, C.;
764 Rogowsky, P. M. Molecular characterisation of two novel maize LRR receptor-like kinases, which
765 belong to the SERK gene family. *Planta* **2001**, 213 (1), 1-10.

766 (25) Lin, Y.; Liu, H.; Waraky, A.; Haglund, F.; Agarwal, P.; Jernberg-Wiklund, H.; Warsito, D.;
767 Larsson, O. SUMO-modified insulin-like growth factor 1 receptor (IGF-1R) increases cell cycle
768 progression and cell proliferation. *J. Cell. Physiol.* **2017**, 232 (10), 2722-2730.

769 (26) Arteca, R. N.; Arteca, J. M. Effects of brassinosteroid, auxin, and cytokinin on ethylene
770 production in *Arabidopsis thaliana* plants. *J. Exp. Bot.* **2008**, 59 (11), 3019-26.

771 (27) Zhu, X. F.; Yuan, P.; Zhang, C.; Li, T. Y.; Xuan, Y. H. RAVL1, an upstream component of
772 brassinosteroid signalling and biosynthesis, regulates ethylene signalling via activation of EIL1 in rice.
773 *Plant Biotechnol. J.* **2018**, 16 (8), 1399-1401.

774 (28) Guo, Y. F.; Shan, W.; Liang, S. M.; Wu, C. J.; Wei, W.; Chen, J. Y.; Lu, W. J.; Kuang, J. F.
775 MaBZR1/2 act as transcriptional repressors of ethylene biosynthetic genes in banana fruit. *Physiol*
776 *Plant* **2019**, 165 (3), 555-568.

777 (29) Qin, Y. M.; Zhu, Y. X. How cotton fibers elongate: a tale of linear cell-growth mode. *Curr. Opin.*
778 *Plant Biol.* **2011**, 14 (1), 106-11.

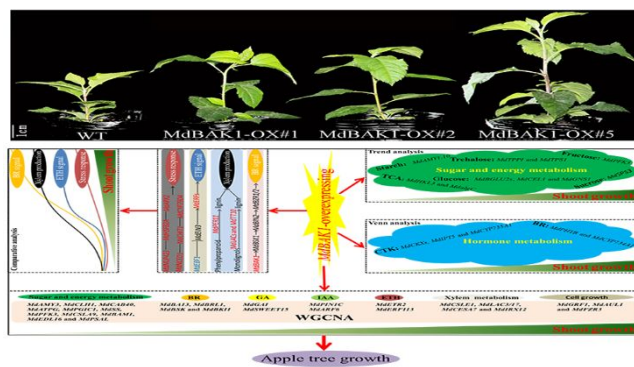
779 (30) Kuroha, T.; Nagai, K.; Gamuyao, R.; Wang, D. R.; Furuta, T.; Nakamori, M.; Kitaoka, T.;
780 Adachi, K.; Minami, A.; Mori, Y.; Mashiguchi, K.; Seto, Y.; Yamaguchi, S.; Kojima, M.; Sakakibara,
781 H.; Wu, J.; Ebana, K.; Mitsuda, N.; Ohme-Takagi, M.; Yanagisawa, S.; Yamasaki, M.; Yokoyama, R.;

- 782 Nishitani, K.; Mochizuki, T.; Tamiya, G.; McCouch, S. R.; Ashikari, M. Ethylene-gibberellin signaling
783 underlies adaptation of rice to periodic flooding. *Science* **2018**, 361 (6398), 181-186.
- 784 (31) Ye, X.; Fu, M.; Liu, Y.; An, D.; Zheng, X.; Tan, B.; Li, J.; Cheng, J.; Wang, W.; Feng, J.
785 Expression of grape ACS1 in tomato decreases ethylene and alters the balance between auxin and
786 ethylene during shoot and root formation. *J. Plant Physiol.* **2018**, 226, 154-162.
- 787 (32) Yu, J. Q.; Huang, L. F.; Hu, W. H.; Zhou, Y. H.; Mao, W. H.; Ye, S. F.; Nogues, S. A role for
788 brassinosteroids in the regulation of photosynthesis in *Cucumis sativus*. *J. Exp. Bot.* **2004**, 55 (399),
789 1135-43.
- 790 (33) Peleg, Z.; Reguera, M.; Tumimbang, E.; Walia, H.; Blumwald, E. Cytokinin-mediated
791 source/sink modifications improve drought tolerance and increase grain yield in rice under water-stress.
792 *Plant Biotechnol. J.* **2011**, 9 (7), 747-58.
- 793 (34) Best, N. B.; Hartwig, T.; Budka, J.; Fujioka, S.; Johal, G.; Schulz, B.; Dilkes, B. P. *nana plant2*
794 Encodes a Maize Ortholog of the Arabidopsis Brassinosteroid Biosynthesis Gene DWARF1,
795 Identifying Developmental Interactions between Brassinosteroids and Gibberellins. *Plant Physiol.* **2016**,
796 171 (4), 2633-47.
- 797 (35) Unterholzner, S. J.; Rozhon, W.; Papacek, M.; Ciomas, J.; Lange, T.; Kugler, K. G.; Mayer, K. F.;
798 Sieberer, T.; Poppenberger, B. Brassinosteroids Are Master Regulators of Gibberellin Biosynthesis in
799 Arabidopsis. *Plant Cell* **2015**, 27 (8), 2261-72.
- 800 (36) Bai, M. Y.; Shang, J. X.; Oh, E.; Fan, M.; Bai, Y.; Zentella, R.; Sun, T. P.; Wang, Z. Y.
801 Brassinosteroid, gibberellin and phytochrome impinge on a common transcription module in
802 Arabidopsis. *Nat. Cell Biol.* **2012**, 14 (8), 810-7.

- 803 (37) Lee, H. S.; Kim, Y.; Pham, G.; Kim, J. W.; Song, J. H.; Lee, Y.; Hwang, Y. S.; Roux, S. J.; Kim,
804 S. H. Brassinazole resistant 1 (BZR1)-dependent brassinosteroid signalling pathway leads to ectopic
805 activation of quiescent cell division and suppresses columella stem cell differentiation. *J. Exp. Bot.*
806 **2015**, 66 (15), 4835-49.
- 807 (38) Cho, H.; Ryu, H.; Rho, S.; Hill, K.; Smith, S.; Audenaert, D.; Park, J.; Han, S.; Beeckman, T.;
808 Bennett, M. J.; Hwang, D.; De Smet, I.; Hwang, I. A secreted peptide acts on BIN2-mediated
809 phosphorylation of ARFs to potentiate auxin response during lateral root development. *Nat. Cell Biol.*
810 **2014**, 16 (1), 66-76.
- 811 (39) Argyros, R. D.; Mathews, D. E.; Chiang, Y. H.; Palmer, C. M.; Thibault, D. M.; Etheridge, N.;
812 Argyros, D. A.; Mason, M. G.; Kieber, J. J.; Schaller, G. E. Type B response regulators of Arabidopsis
813 play key roles in cytokinin signaling and plant development. *Plant Cell* **2008**, 20 (8), 2102-16.
- 814 (40) Wang, S. S.; Liu, Z. Z.; Sun, C.; Shi, Q. H.; Yao, Y. X.; You, C. X.; Hao, Y. J. Functional
815 characterization of the apple MhGAI1 gene through ectopic expression and grafting experiments in
816 tomatoes. *J. Plant Physiol.* **2012**, 169 (3), 303-10.
- 817 (41) Ma, C.; Lu, Y.; Bai, S.; Zhang, W.; Duan, X.; Meng, D.; Wang, Z.; Wang, A.; Zhou, Z.; Li, T.
818 Cloning and characterization of miRNAs and their targets, including a novel miRNA-targeted
819 NBS-LRR protein class gene in apple (Golden Delicious). *Mol. Plant* **2014**, 7 (1), 218-30.

820

821



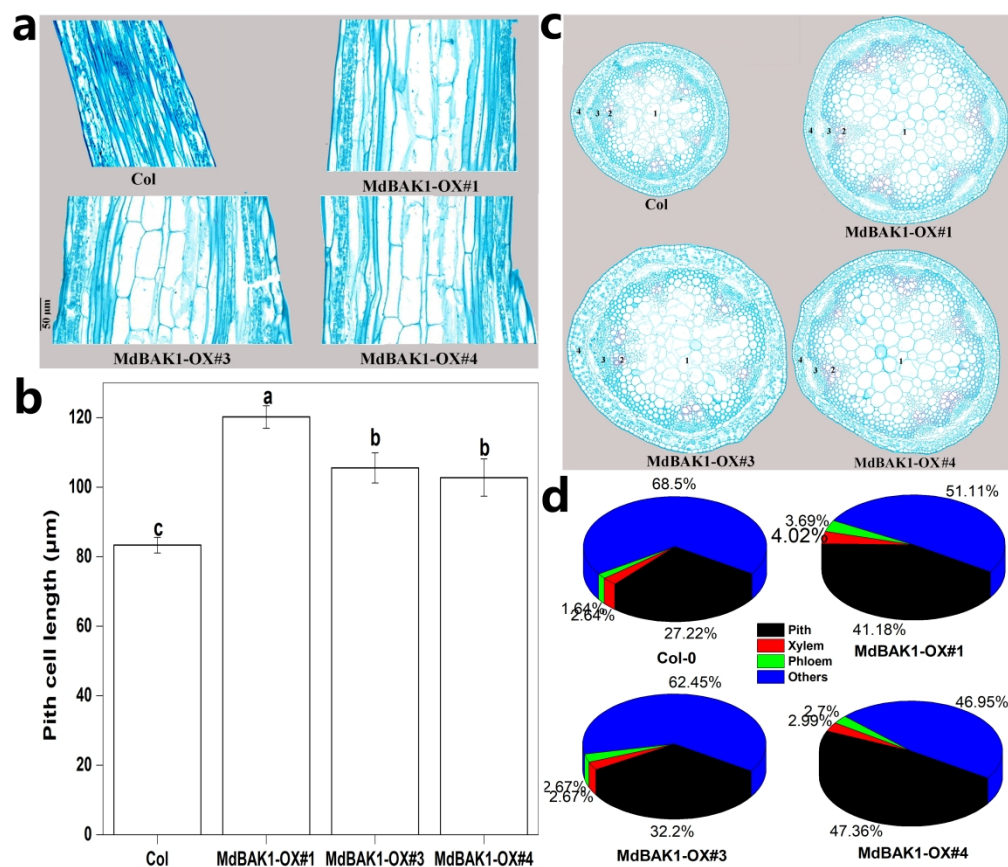


Figure 1. Anatomical analysis of the *Arabidopsis thaliana* stem. (a) Partial longitudinal sections. (b) Pith cell length of WT, MdBAK1-OX#1, MdBAK1-OX#3, and MdBAK1-OX#4. (c) Stem cross-section. (d) Proportion of stem cross-section represented by the xylem, phloem, pith, and other components (includes the epidermis, cortex, and interfascicular cambium). 1: pith; 2: xylem; 3: phloem; 4: cortex. Values are presented as the mean \pm standard error of three replicates.

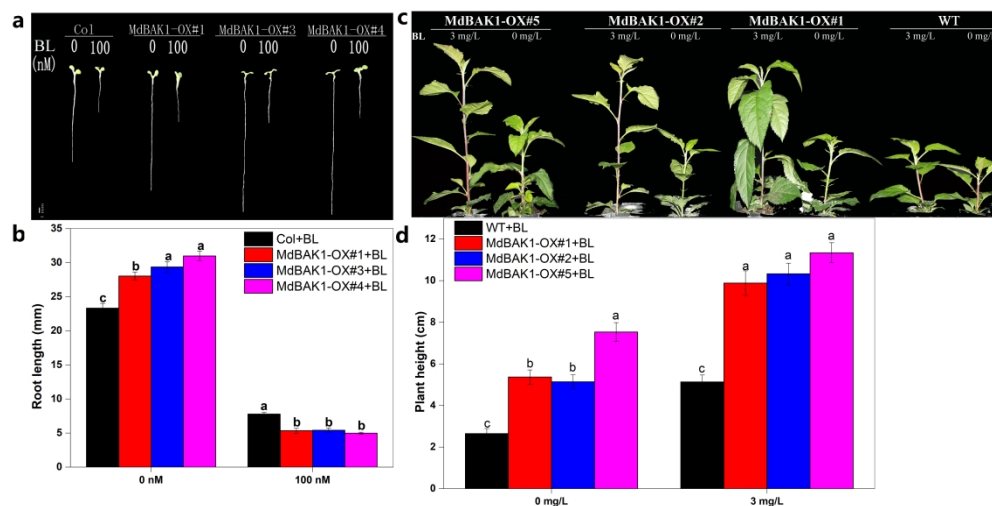


Figure 2. Analysis of the BR sensitivity of WT and transgenic lines.

(a) Phenotype of 7-day-old BR-treated seedlings grown under light. (b) Root length of WT and transgenic *Arabidopsis thaliana* at 7 days after a BR treatment. Values are presented as the mean \pm standard error of nine replicates. (c) Phenotype of WT and transgenic apple trees treated with BR. (d) Plant height of WT and transgenic apple trees treated with BR. Three biological replicates (three trees per replicate) and three technical replicates were analyzed. Different letters indicate significant differences at the 0.05 level.

496x248mm (300 x 300 DPI)

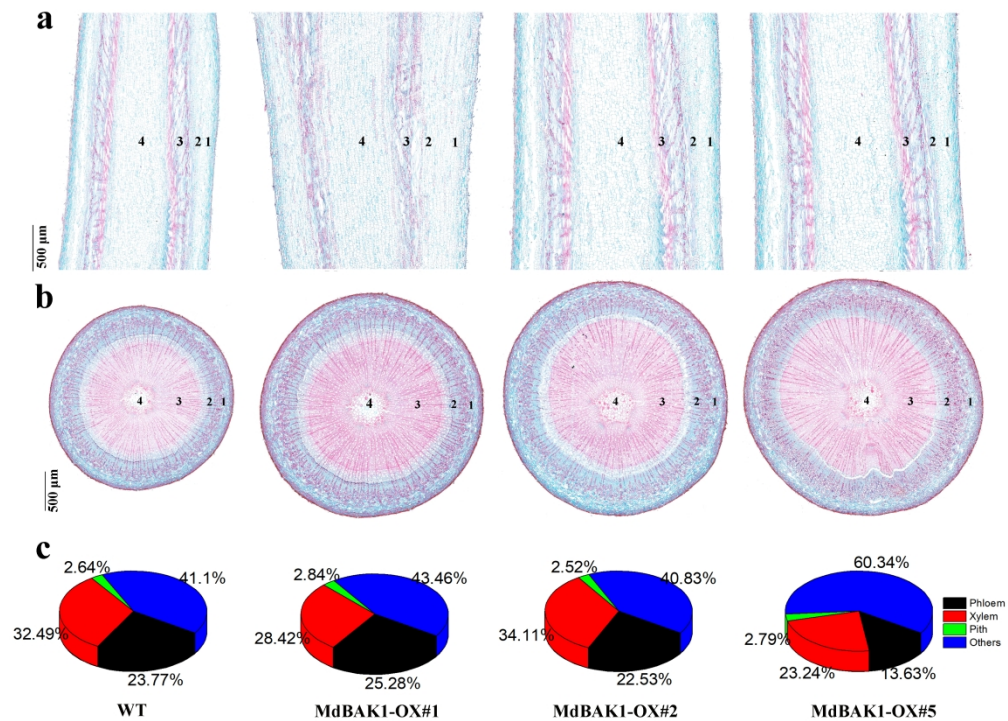


Figure 3. Anatomical analysis of the apple tree stem. (a) Longitudinal stem section. (b) Stem cross-section. (c) Proportion of the stem cross-section represented by the xylem, phloem, pith, and other components (includes the epidermis, cortex, and interfascicular cambium). 1: cortex; 2: phloem; 3: xylem; 4: pith. Three biological replicates (three trees per replicate) of the WT and transgenic lines were analyzed.

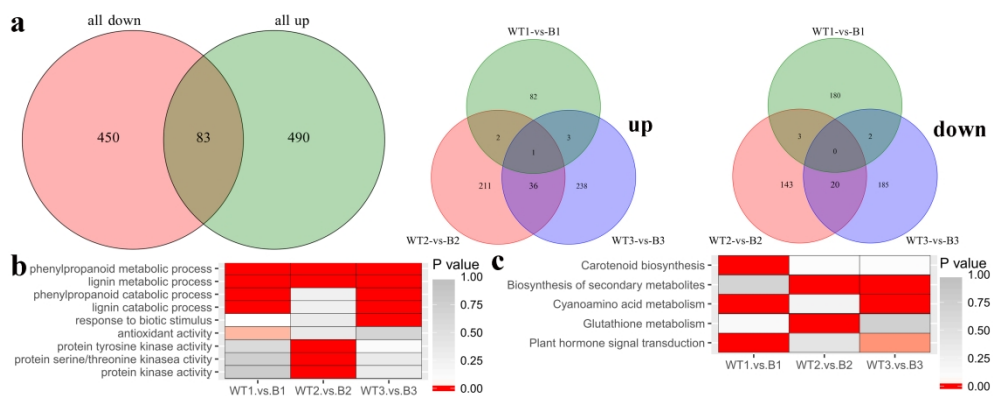


Figure 4. Analysis of the functional enrichment of the DEGs between WT and B plants. (a) Venn diagrams of all genes exhibiting up- or downregulated expression between WT and B plants. (b) Results of the GO enrichment analysis of the DEGs between WT and B plants. (c) Results of the KEGG pathway enrichment analysis of the DEGs between WT and B plants.

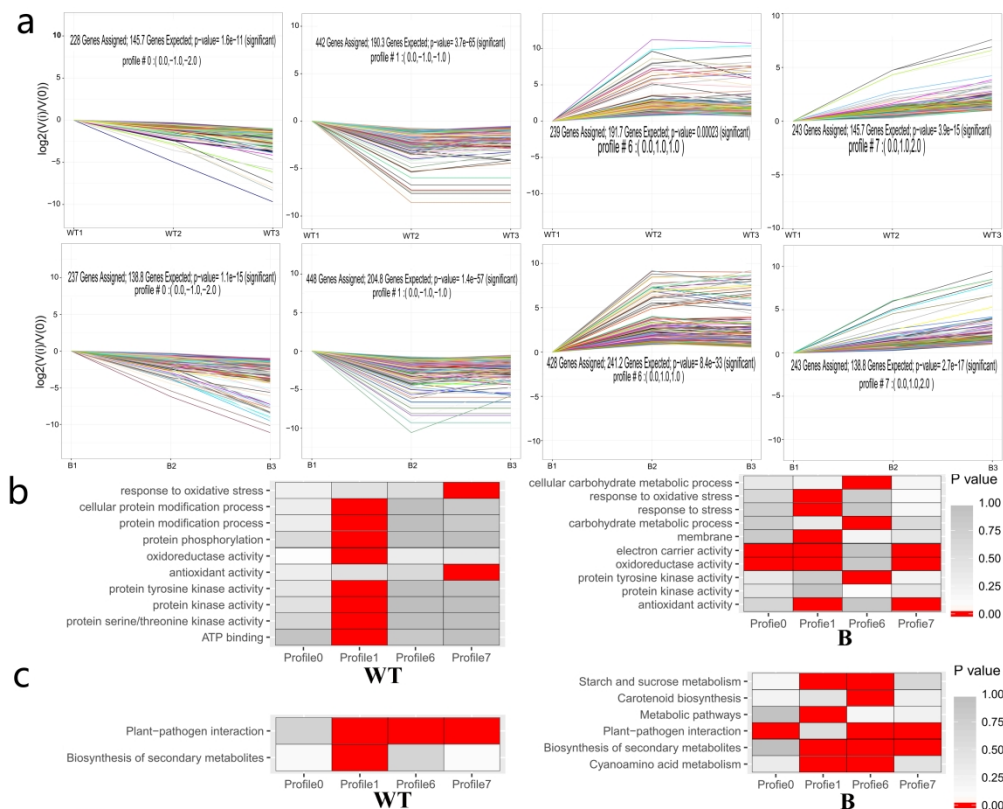


Figure 5. Gene expression patterns and enrichment of GO terms and KEGG pathways across three time-points in WT and B plants. (a) Gene expression patterns at three time-points in WT and B plants predicted with STEM software. The number of genes and p-values for each pattern are indicated in the frame. (b) Results of the GO enrichment analysis of important processes in WT and B plants. (c) Results of the KEGG pathway enrichment analysis of important processes in WT and B plants. The p-value was used to indicate the significance of the most represented GO and KEGG Slim terms. Significant p-values are indicated in red, whereas non-significant p-values are indicated in dark gray.

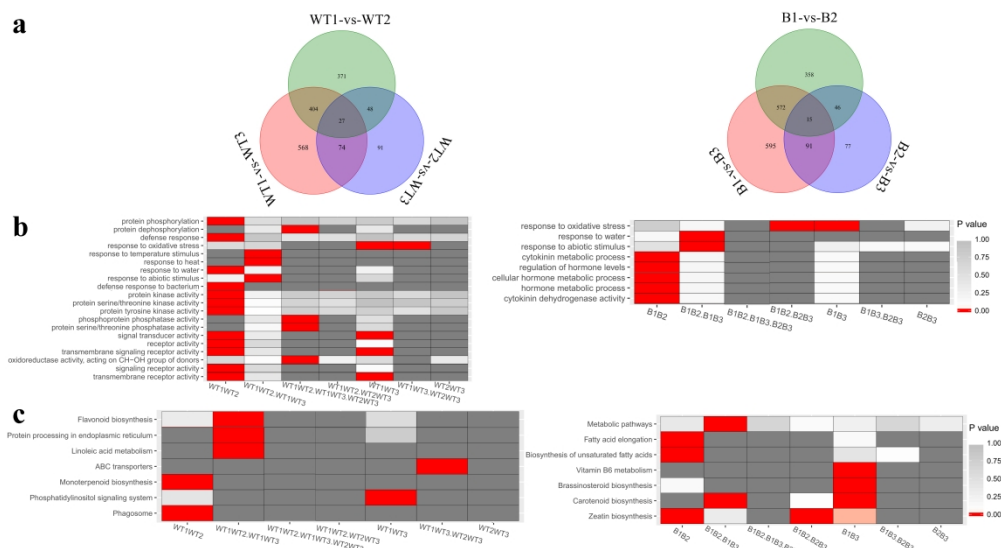


Figure 6. Venn analysis of DEGs over time in WT and B. (a) Number of DEGs in the WT and B plants. (b) Clusters of annotated GO terms for the DEGs in the WT and B plants. (c) Results of the KEGG pathway enrichment analysis of the DEGs in the WT and B plants. The significance of the most represented terms is indicated by a p-value. Significant p-values are indicated in red, whereas non-significant p-values are indicated in dark gray.

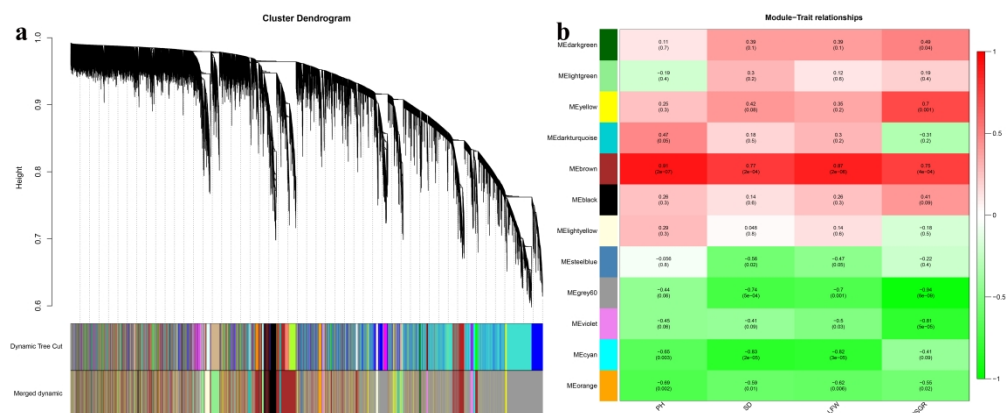


Figure 7. Weighted gene co-expression network analysis (WGCNA) of genes identified in the WT and B plants over three developmental stages. (a) Twelve modules of co-expressed genes are shown in a hierarchical cluster tree. A major tree branch represents a module. Modules in designated colors are presented in the lower panel. (b) Module-trait relationships. The 12 modules are provided in the left panel. The module-trait correlation, from -1 (green) to 1 (red), is indicated with the color scale on the right. Each column presents the experimental traits, and their association with each module is represented by a correlation coefficient and a p-value in parentheses.

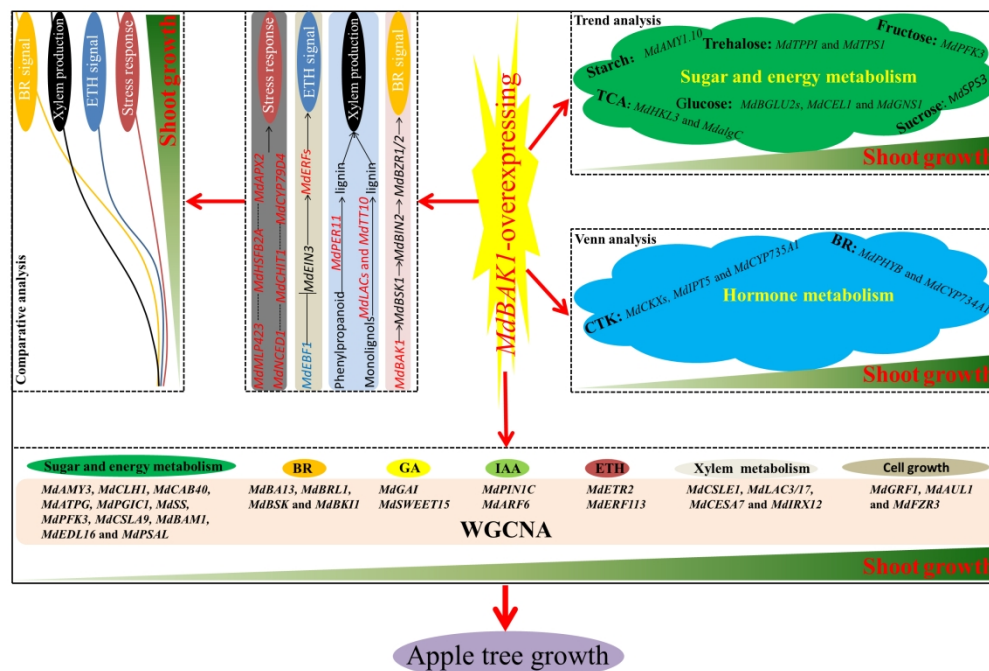


Figure 8. Proposed model for the MdBak1 overexpression-mediated regulation of apple tree growth. A comparative analysis revealed that BR signaling, xylem production, ETH signaling, and stress responses are activated during shoot growth, and are respectively indicated with orange, black, blue and carmine curves. Arrows (positive regulation) or blocked arrows (negative regulation) represent crucial metabolic steps. The expression levels of genes in red or blue are respectively upregulated or downregulated in B. The trend and Venn analyses indicated that sugar and energy and hormone metabolic activities are enriched over time. Crucial metabolic pathways and genes based on a WGCNA are indicated.